Nano World Journal

https://doi.org/10.17756/nwj.2024-s1-001

Research Article

Open Access

Mechanical Characterization of Magnesium-Hydroxyapatite Surface Composite Fabricated by Friction Stir Processing

Syeda Romana and Nagaveni Thallapalli*

Department of Mechanical Engineering, University College of Engineering, Osmania University, Hyderabad, Telangana, India

***Correspondence to:**
Nagaveni Thallapalli
Department of Mechanical Engineering,
University College of Engineering,
Osmania University,
Hyderabad, Telangana, India.
E-mail: nagaveni.t@uceou.edu

Received: January 03, 2024
Accepted: March 04, 2024
Published: March 07, 2024

Citation: Romana S, Thallapalli N. 2024. Mechanical Characterization of Magnesium-Hydroxyapatite Surface Composite Fabricated by Friction Stir Processing. *NanoWorld J* 10(S1): S01-S06.

Published by United Scientific Group

Abstract

Usage of surface metal composites in the field of orthopedics is increasing nowadays due to their biocompatibility. But fabrication of surface composites with all the desired properties is the major challenge. The primary objective of this research is to produce a surface composite of a magnesium AZ31B alloy reinforced with different volume fractions (0%, 5%, 10%, 15%, 20 and 25%) of hydroxyapatite (HA) microparticles using friction stir processing (FSP). This work demonstrates that variation of uniform distribution of HA particles (HAP) is observed in all volume percentage of AZ31B-HA powder composites. As percentage of reinforcement decreases up to 10% of volume tensile strength is decreasing but above that tensile strength is increasing. Above 10% HAP volume percentage addition of more HAP has no effect on wear coefficient. The minimum value of wear coefficient is observed at 20% HAP volume percentage with the value of 0.2728 μg/N-m which is 81.68% less than 0% HAP composition. As the volume percentage of HAP increasing from 0% to 15% around 27.61% increase in the hardness value is observed and decrease in hardness value from 15% to 25% around 17.11% is observed. Rockwell hardness values are more at advancing side than retreating side in all volume percentages of HAP.

Keywords

Orthopedics, Biocompatibility, Magnesium metal matrix composite, Hydroxyapatite, Friction stir processing

Introduction

The advantages of magnesium as a temporary, biodegradable implant have gained attention in recent years because to its unique biodegradation in combination with suitable mechanical qualities, high bioactivity, and biocompatibility. This makes magnesium a promising option to polymers. Additionally, because magnesium and its alloys have an elastic modulus close to that of natural bone, they can be used as implants to prevent the stress shield effect during implantation [1]. While the development of magnesium-based biomaterials is hampered and slowed by a variety of difficulties, biodegradable magnesium and its alloys are potentially appealing for the orthopedic profession [2]. The main problem with magnesium is that it corrodes quickly, especially in environments rich in life. In order to keep functioning for a long enough period of time while damaged tissue heals, it is necessary to make a significant effort to minimize the pace of magnesium corrosion [3]. In the literature, numerous techniques have been used to address this problem. Investigating the creation of environmentally friendly coatings and surface modification receives the most focus. Coatings for biodegradable materials must meet the same biocompatibility and biodegradability standards as the base substrate.

In-situ precipitates with the smallest particle size of the order of 0.8 m are

produced after a single pass FSP of the AZ31 alloy, according to Babu et al. [4]; these precipitates can be further refined during a double pass FSP and also in subsequent passes. The spindle speed and feed rate combination of 800 rpm and 40 mm/min produces the lowest precipitate size. The comparable Vickers hardness value is 63, which is roughly 50% more than that of the base metal. By using FSP, Wang et al. [5] successfully created AZ31/ZrO_2 nanocomposites with good homogeneity and investigated their mechanical, biological, and electrochemical corrosion capabilities. The AZ31/ZrO_2 composite material achieves homogeneity, densification, and grain refinement after FSP when results are compared to the base metal.

To study the impact of second phase particle addition to composite, Mosayebi et al. [6] processed a magnesium composite comprising rare earth with silicon carbide reinforcement. This was attributed to the functioning of the mechanism for particle-stimulated nucleation and the pinning action of silicon carbide particles. The effects of HA ($Ca_{10}(PO_4)_6OH_2$), a ceramic that resembles bone mineral, on the bio-corrosion behavior of AZ31B-magnesium alloy were investigated [7]. The magnesium matrix was mixed with HA at various weight percentages (5, 10, and 20 wt.%). When compared to untreated AZ31B, the results showed that the composites had improved corrosion resistance, which was due in large part to the FSP considerable grain refinement.

Kasaeian-Naeini and colleagues [8] created magnesium/HA bio-composites and investigated the behavior of magnesium/1 wt.% and magnesium/2.5 wt.% HA during high-temperature deformation. The reinforced nano-HAP with magnesium composite were analyzed by Sunil et al. [9], who also looked at the composite's grain structure, corrosion behavior, and cell adhesion. They reported that after FSP, the nano-HAP were discovered to be disseminated in pure magnesium. Due to the produced fine grain structure, wettability for the composite was seen to be significantly elevated. Grain refinement and greater biomineralization both significantly improved corrosion resistance as determined by electrochemical tests on corrosion behavior [9, 10].

Patel et al. [11] studied on "Enhancing grain refinement and corrosion behavior in AZ31B-magnesium alloy via stationary shoulder FSP", came to the conclusion that the shoulder's fixed action creates a fine-grained microstructure that is evenly distributed across stir zone, which improves the corrosion behavior. Many researchers thought of using HA as a coating material on the surface of magnesium to increase bioactivity and corrosion resistance using different methods. As a result, the current work advances on prior work by additively creating the layer-structured coatings of HA on AZ31B-magnesium alloy.

Ahirwar et al. [12] studied a wide range of orthopedic condition, such as fracture fixation, total bone replacement, joint arthrodesis, dental screws, and others, can now be treated thanks to significant research and development in the field of biomedical implants. Crucially, the interaction between a bioimplant and its host tissue is determined by its surface characteristics as well as its bulk characteristics.

Different surface coatings using silver-based nanocomposite, using nano-titanium dioxide, and titanium dioxide-based metal nanocomposites, zinc oxide-based nanocomposite, silver-CeSZ nanocomposite. Thus, coated nanomaterials have the potential alter the surface of different metallic materials so that they can be used in orthopedic applications. The preparation and deposition of nanomaterials on bioimplant surfaces, however, require caution due to factors such as control over the nanomaterial size distribution, bonding with the implant surface, and thickness of deposited nanomaterial.

Most of the research work has been reported on magnesium with reinforcement such as silicon, carbide, alumina, etc. Magnesium composite reinforced with HAP could be the best composite due to their individual biocompatibility and bioactivity properties [13]. But the work related to magnesium AZ31B reinforced with HA is very limited. Magnesium and HAP are proved to be the best materials individually in the field of orthopedics.

This magnesium AZ31B and HAP composite can be the potential material in place of bone material. But the magnesium is heavily corrosive nature so the use of this composite limited [14]. An attempt can be made on this composite to enhance the properties of the material using FSP so that it is useful in an economic way. There is not much work related to tensile behavior, wear rate and hardness of AZ31B/HAP composite and so this work is intended to fabricate a surface composite of magnesium AZ31B and HAP and experimentally investigate the effects of variation in volume percentage of reinforcement on microstructure and mechanical properties.

Materials and Method

Two magnesium AZ31B alloy plates are chosen as matrix material as shown in the figure 1 with 150 mm x 150 mm x 6 mm. HAP is used as reinforcement in this study of 20-micron size and of 99% purity (Purchased from Vedayuktha Pvt. Ltd.). Due to its already established biocompatibility and its resemblance to genuine bone in terms of chemical composition and structural organization, HAP was an obvious choice during the earliest stages of magnesium-based biomaterial development. HAP can improve the composite's biocompatibility while also improving the composite's corrosion resistance and mechanical attributes.

Two number of tools used for the purpose of friction stir in this work. Tool material selected is H13 steel. One tool is made as pin less tool with 20 mm shoulder diameter. This tool is useful for closing the grooves after filling the powder in grooves. This is to avoid spillage of powder during the process

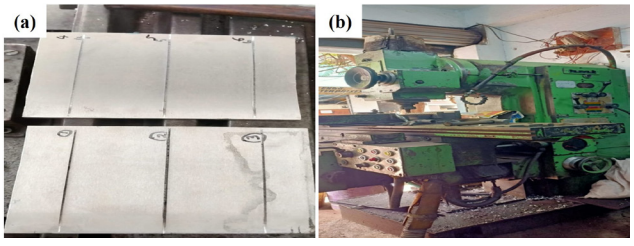

Figure 1: (a) Sample with grooves and **(b)** FSP set up.

and to avoid clustering of powder at one place due to the force given by pin while traversing on the adjacent powder. Another tool is designed with 20 mm shoulder diameter and 4 mm pin diameter and a pin length of 5 mm is chosen. This pin does the actual processing.

First grooves are closed with pin less tool again processing is done on the same sample with this pinned tool. To perform the FSP, two plates of 150 x 150 mm were taken, and it is marked for 50 mm width that the plate is divided into three parts, with these three experiments can be done on each plate.

In these plates square grooves of 4 mm depth with varying width as per volume percentage (0, 5, 10, 15, 20 and 25%) of the reinforcing material were made with mill cutters as shown in figure 1a. The relation between the tool pin dimension, groove dimension and volume percentage of the powder is given below.

$$\text{Volume Fraction} = \frac{\text{Area of Groove}}{\text{Projected Area of Pin}} \times 100$$

Area of Groove = Groove width x Groove depth

Projected Area of Pin = Pin length x Pin diameter

As of the powder to be filled = Density of powder x Volume

One tool is made as pin less tool with 20 mm shoulder diameter and is used for closing the grooves after filling the powder in grooves. Another tool is designed with 20 mm shoulder diameter and 4 mm pin diameter and a pin length of 5 mm is chosen and By keeping tool rotational speed as 1200 rpm, axial force 5 kN and tool traverse speed as 40 mm/min processing is done on the sample.

According to the above relation width of groove and amount of powder to be filled in each groove are determined. A total of six samples are prepared along with a base plate sample. Sample after making groove is shown in figure1a. Prepared sample is fixed on FSP machine with the help fixtures as shown in figure 1b and pinless tool is fixed in tool post. By keeping tool rotational speed as 1200 rpm, axial force 5 kN and tool traverse speed as 40 mm/min processing is done on the sample. After completing the processing with pinless tool, tool is removed from the tool post and placed pinned tool in the tool post. With the pinned tool processing is done on all samples as shown in figure 2a. Samples for tensile, wear, corrosion, and microstructural analysis were acquired on wire EDM after the AZ31B-HA composite was produced. Figure 2b presents a schematic illustration of the area where the test sample was acquired.

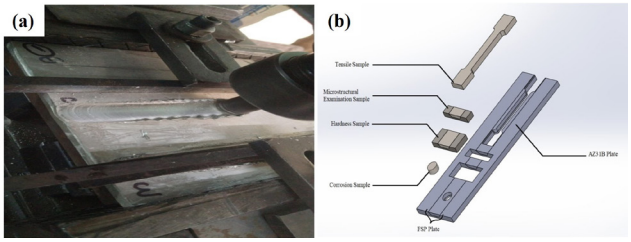

Figure 2: (a) Sample during FSP and **(b)** Schematic illustration of the area where test samples are acquired.

Characterization

Tensile specimens have been cut on the wire EDM machine as per ASTME0008M-04 standard as discussed. Specimens of dimensions 8 mm diameter as per ASTM G009-04A standard were cut from the middle part of FSP zone to carry out dry sliding wear test. Figure 2 shows samples which were cut from friction stir zone. The wear test was conducted at room temperature in an unlubricating environment temperature as per ASTM G99-O4A standards. The wear characteristics of specimens pressed to a rotating steel disc counterpart constructed of EN 24 grade were examined using a pin-on-disc device made by DUCOM. After each test, the steel disc was cleaned with acetone and polished with 240 grit emery sheets. Polished specimen pin was fixed to steel disc in a stationary position, and the disc rotated in accordance with the input speed and time as required. Applying normal force is the duty of the cantilever beam on which the pin is supported. In order to quantify weight loss from which wear rate is estimated, pins are weighed before and after each test in a precision-electronic scale (accuracy 0.1 mg).

Results and Discussion

Microstructural analysis

Observation from these microstructure graphs show that microstructure is observed clearly in all samples and also there is a uniform distribution of HAP in all percentage of volume composites. But as compared to the samples from AZ31B-0% HAP to AZ31B-10% HAP volume percentage composites more than AZ31B-10% HAP volume composites shows the agglomeration of particles which may affect the mechanical properties irrespective of the effect of other parameters (Figure 3). Porosity is not observed in all the samples which is good for analysing the effect of properties accurately. As percentage of volume concentration of HAP is increased there is a distortion is observed in the grain structure.

Figure 4 show scanning electron microscope images of the interlock friction stir sample with various HAP contents. Due to the varying weight percentages of the composition of the HAP content, the microstructure at the weld zone was asymmetric. Figure 5 presents element composition analysis.

Tensile test

From the above values, it is observed that tensile strength values of all samples are higher than the base metal magensium-AZ31B alloy tensile strength whose ultimate tensile strength is 260 MPa. Furthermore, it is observed that as the volume percentage of HAP is increasing till 15% in AZ31B metal matrix ultimate tensile strength values have decreased. The same trend is observed in yield strength also but till 10% HAP composite. The reason for decrease in tensile strength initially is due to grain refinement occurred during the process. The temperature induced while processing the samples increases the grain size which reduces the tensile strength. Maximum tensile strength value 475.56 MPa is observed with AZ31B-0% HAP composite which is 82.91% higher than

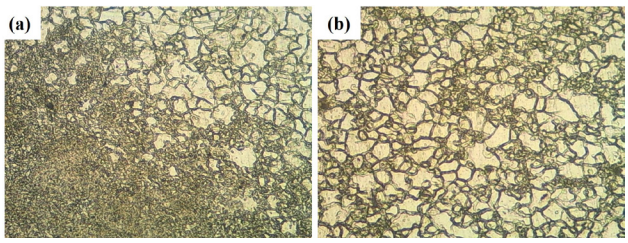

Figure 3: Microstructure of the **(a)** Heat affected zone and **(b)** Thermo-mechanical affected zone.

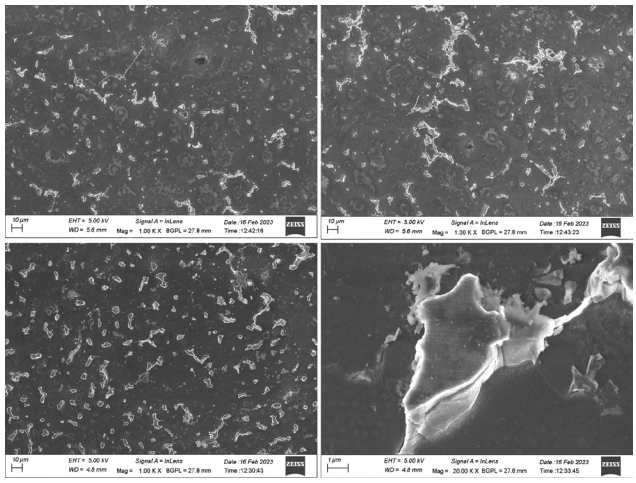

Figure 4: Scanning electron microscope images showing the microstructure of FSP specimens processed by different HAP content.

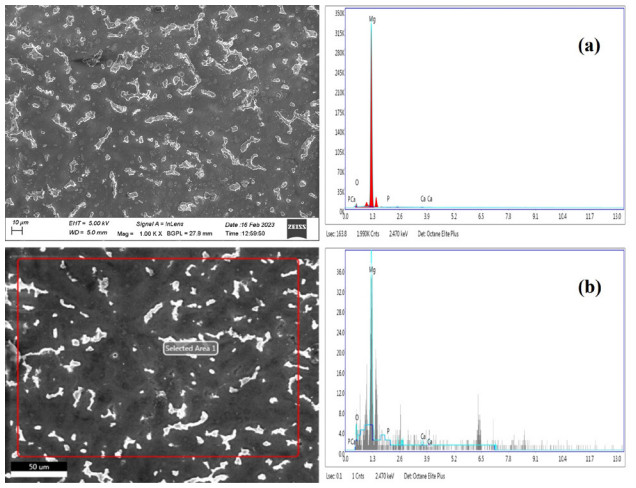

Figure 5: Energy dispersive X-ray spectroscopy analysis for **(a)** AZ31B-5% HAP composite and **(b)** AZ31B-15% HAP composite.

base material. Further increase in the tensile yield strength value is due to precipitates formed during the processing. This can be explained by Orowan strengthening mechanism [15]. As per this mechanism as concentration of precipitates increases tensile strength values increases. The same trend is observed with yield strength values also. These values are taken from the digital reports of the test. The percentage of elongation, yield strength, and ultimate tensile strength are reported in the table 1. The graphs of stress vs strain for various AZ31B-HAP composites are drawn below in figure 6 which were taken from the reports.

Table 1: Tensile test values.

S. No.	Volume percentage of sample (%)	Ultimate tensile strength (MPa)	Yield strength (MPa)	Percentage of elongation (%)
1	0	477.78	229.31	11.6
2	5	448.89	227.04	11.56
3	10	330.56	225.72	4.26
4	15	378.89	227.98	6.2
5	20	431.11	230.02	8.2
6	25	379.44	225.59	9.4

Ultimate tensile strength and percentage of elongation versus varying HAP composition graphs are drawn in figure 7. As the volume percentage of HAP increases till 10% percentage of elongation values are decreasing till 10% HAP composite then beyond 10% HAP in AZ31B metal matrix as the volume percentage of HAP increasing percentage of elongation is increasing. The reason for this trend is due to first it is decreasing due to difficulty in the movement of dislocation because of the HAP. Further increase in the elongation is due to formation of precipitates which comes out of the grains which reduces the resistance for deformation so that dislocation movement becomes easier so the material will have longer elongation.

Rockwell hardness test

Rockwell hardness values are taken at five different zones from the centreline of the processed zone and the values are tabulated designated as -2, -1, 0, +1, and +2 from advancing zone to retreating zone. The graph of Rockwell hardness vs distance from center line are drawn for different HAP volume concentration in the figure 8. Observations made from the above results are average hardness value is increased due to FSP compared to AZ31B base material. This is due to grain refinement happening during processing. As the volume percentage of HAP increasing from 0% to 15% around 27.61% increase in the hardness value is observed. This is due to uniform distribution of HAP in the matrix. Dislocation motion is resisted by the homogeneous distribution, which also changes the direction in which they move. But there is a decrease in hardness value as the volume percentage of HAP increasing from 15% to 25% which is around 17.11%. This might be due to agglomeration of HAP formed as it is not having sufficient material flow.

Another interesting observation is Rockwell hardness values are more at advancing side than retreating side in all volume percentages of HAP. It is due to material flow is difficult in advancing side than retreating side. In advancing side material is trying to flow backward and tool tries to forge the material in forward direction. But this forging effect is not observed in retreating side because at retreating side material flow direction and tool direction are same. Due to this forging effect average hardness values are higher at advancing side than retreating side as there is no forging effect at retreating side.

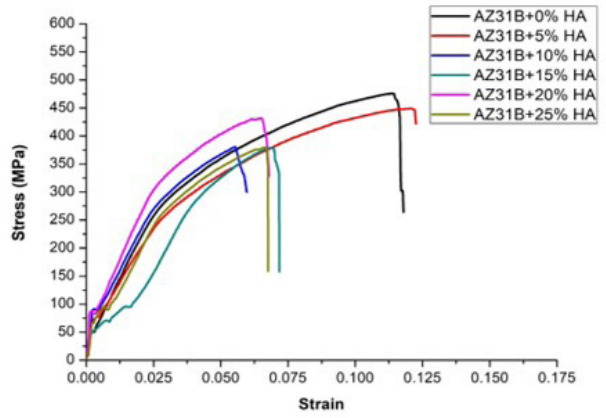

Figure 6: Stress-strain curves for AZ31B-HAP composites specimens containing different HAP content.

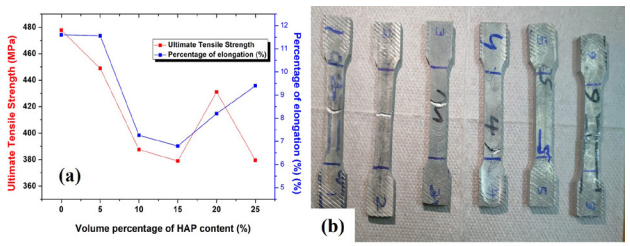

Figure 7: (a) Elongation and ultimate tensile strength variations of AZ31B-HAP composites specimens containing different HAP content. **(b)** Specimens after performing tensile test.

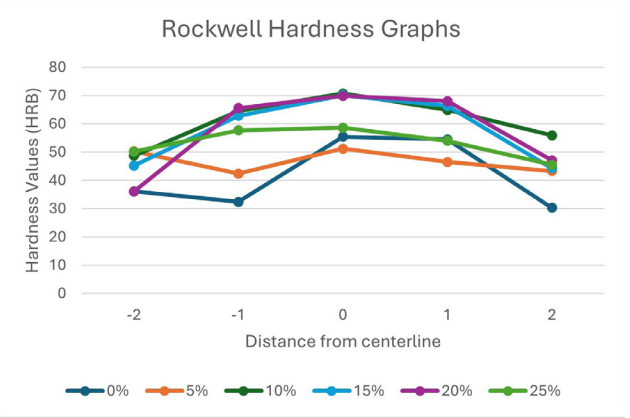

Figure 8: Hardness values for various AZ31B-HAP composition at various points.

Wear test

Weight of the samples before and after the experiments is noted down. Wear coefficient values are found out from the formulas. All the results are tabulated in the table 2.

From the values it is observed that wear coefficient values are decreasing as the volume percentage of HAP increasing. This is due to distorted AZ31B grains due to added HAP. Hardness values have increased in this composition which shows decrease in the wear coefficient values is an obvious effect. But after 10% HAP volume percentage there rise and fall of wear coefficient values which is more or less equal neglecting other effects. From this it can be concluded that addition of more reinforcement will not have any effect on the wear coefficients. The minimum value of wear coefficient is observed at 20% HAP volume percentage with the value of 0.2728 µg/N-m which is 81.68% less than 0% HAP composition.

Table 2: Wear test values for various AZ31B-HAP compositions.

HAP volume fraction	Weight before (g)	Weight after (g)	Difference in weight (g)	Wear coefficient (µg/N-m)
0%	4.0793	4.0662	0.0131	1.489235612
5%	4.4535	4.441	0.0125	1.421026347
10%	4.4559	4.4515	0.0044	0.500201274
15%	4.4926	4.4867	0.0059	0.670724436
20%	4.5914	4.589	0.0024	0.272837059
25%	4.3949	4.3906	0.0043	0.488833063

Conclusions

Magnesium AZ31B-HAP surface composites of various compositions have been successfully produced utilizing FSP in the current investigation. Researchers have looked at the impact of the FSP on the microstructure, tensile strength, microhardness, and wear. From the results of the experiment, the following conclusions were drawn.

- Uniform distribution of HAP is observed in all compositions of AZ31B-HAP composites.
- As percentage of reinforcement decreases up to 10% of volume tensile strength is decreasing but above that tensile strength is increasing.
- Maximum tensile strength value 475.56 MPa is observed with AZ31B-0% HAP composite which is 82.91% higher than base material.
- Above 10% HAP volume percentage addition of more HAP has no effect on wear coefficient.
- The minimum value of wear coefficient is observed at 20% HAP volume percentage with the value of 0.2728 µg/N-m which is 81.68% less than 0% HAP composition.
- As the volume percentage of HAP increasing from 0% to 15% around 27.61% increase in the hardness value is observed and decrease in hardness value from 15% to 25% around 17.11% is observed.
- Rockwell hardness values are more at advancing side than retreating side in all volume percentages of HAP.

Acknowledgments

None.

Conflict of Interest

None.

References

1. Yazdimamaghani M, Razavi M, Vashaee D, Moharamzadeh K, Boccaccini AR, et al. 2017. Porous magnesium-based scaffolds for tissue engineering. *Mater Sci Eng C* 71: 1253-1266. https://doi.org/10.1016/j.msec.2016.11.027

2. Han HS, Loffredo S, Jun I, Edwards J, Kim YC, et al. 2019. Current status and outlook on the clinical translation of biodegradable metals. *Mater Today* 23: 57-71. https://doi.org/10.1016/j.mattod.2018.05.018
3. Peron M, Torgersen J, Berto F. 2017. Mg and its alloys for biomedical applications: exploring corrosion and its interplay with mechanical failure. *Metals* 7(7): 252. https://doi.org/10.3390/met7070252
4. Babu J, Anjaiah M, Mathew A. 2018. Experimental studies on Friction stir processing of AZ31 magnesium alloy. *Mater Today Proc* 5(2): 4515-4522. https://doi.org/10.1016/j.matpr.2017.12.021
5. Wang W, Han P, Peng P, Zhang T, Liu Q, et al. 2020. Friction stir processing of magnesium alloys: a review. *Acta Metall Sin* 33: 43-57. https://doi.org/10.1007/s40195-019-00971-7
6. Mosayebi M, Zarei-Hanzaki A, Tahaghoghi M, Abedi HR, Moshiri A, et al. 2022. Effect of second phase particles on the microstructure and texture of rare earth elements containing magnesium matrix surface-composite produced by friction stir processing. *J Mater Res Technol* 18: 2428-2434. https://doi.org/10.1016/j.jmrt.2022.03.135
7. Liu Y. 2018. Corrosion behaviour of biodegradable Mg-1Ca alloy in simulated body fluid. Faculty of Science and Engineering, The University of Manchester. (Doctoral Dissertation)
8. Kasaeian-Naeini M, Sedighi M, Hashemi R, Delavar H. 2022. An investigation of constitutive modeling and 3D processing maps of Mg/HA composites for orthopedic applications. *J Mater Res Technol* 19: 3894-3915. https://doi.org/10.1016/j.jmrt.2022.06.044
9. Sunil BR, Kumar TS, Chakkingal U, Nandakumar V, Doble M. 2014. Friction stir processing of magnesium–nanohydroxyapatite composites with controlled *in vitro* degradation behavior. *Mater Sci Eng C* 39: 315-324. https://doi.org/10.1016/j.msec.2014.03.004
10. Sunil BR, Reddy GPK, Patle H, Dumpala R. 2016. Magnesium based surface metal matrix composites by friction stir processing. *J Magnes Alloys* 4(1): 52-61. https://doi.org/10.1016/j.jma.2016.02.001
11. Patel V, Li W, Andersson J, Li N. 2022. Enhancing grain refinement and corrosion behavior in AZ31B magnesium alloy via stationary shoulder friction stir processing. *J Mater Res Technol* 17: 3150-3156. https://doi.org/10.1016/j.jmrt.2022.02.059
12. Ahirwar H, Zhou Y, Mahapatra C, Ramakrishna S, Kumar P, et al. 2020. Materials for orthopedic bioimplants: modulating degradation and surface modification using integrated nanomaterials. *Coatings* 10(3): 264. https://doi.org/10.3390/coatings10030264
13. Jhamb S, Matai J, Marwaha J, Goyal A, Pandey A. 2023. A comprehensive analysis on magnesium-based alloys and metal matrix composites for their *in-vitro* biocompatibility. *Adv Mater Process Technol* 9(3): 1249-1282. https://doi.org/10.1080/2374068X.2022.2113521
14. Ali M, Hussein MA, Al-Aqeeli N. 2019. Magnesium-based composites and alloys for medical applications: a review of mechanical and corrosion properties. *J Alloys Compd* 792: 1162-1190. https://doi.org/10.1016/j.jallcom.2019.04.080
15. Eivani AR, Mehdizade M, Chabok S, Zhou J. 2021. Applying multi-pass friction stir processing to refine the microstructure and enhance the strength, ductility and corrosion resistance of WE43 magnesium alloy. *J Mater Res Technol* 12: 1946-1957. https://doi.org/10.1016/j.jmrt.2021.03.021